

Pseudo SU(3) shell model: Normal parity bands in odd-mass nuclei

C. E. Vargas^{1,*}, J. G. Hirsch^{2,†} and J. P. Draayer^{3,‡}

¹ Departamento de Física, Centro de Investigación y de Estudios Avanzados del IPN,
Apartado Postal 14-740 México 07000 DF, México

² Instituto de Ciencias Nucleares, Universidad Nacional Autónoma de México,
Apartado Postal 70-543 México 04510 DF, México

³ Department of Physics and Astronomy, Louisiana State University,
Baton Rouge, LA 70803-4001, USA

November 9, 2018

Abstract

A pseudo shell SU(3) model description of normal parity bands in ^{159}Tb is presented. The Hamiltonian includes spherical Nilsson single-particle energies, the quadrupole-quadrupole and pairing interactions, as well as three rotor terms. A systematic parametrization is introduced, accompanied by a detailed discussion of the effect each term in the Hamiltonian has on the energy spectrum. Yrast and excited band wavefunctions are analyzed together with their B(E2) values.

PACS numbers: 21.60.Fw, 21.60.Cs, 23.20.Lv, 27.70.+q

Keywords: Pseudo SU(3) model, ^{159}Tb , rare earth nuclei, odd-mass nuclei, excitation energies, B(E2) values.

*Electronic address: cvargas@fis.cinvestav.mx; fellow of CONACyT

†Electronic address: hirsch@nuclecu.unam.mx

‡Electronic address: draayer@lsu.edu

1 Introduction

The shell model is a fundamental many-body approach to the study of atomic nuclei [1]. It explains the magic numbers as shell closures and the energy spectra of odd-mass nuclei near closed shells as that of the odd nucleon in a potential well defined by the closed shell nucleons. The remarkable advances in computer power and the use of complex algorithms have allowed for systematic studies of most *sd*- and *fp*-shell nuclei [2]. However, in heavy nuclei is not possible to solve the shell-model problem exactly. Although the fermionic character of the nucleons restricts their allowed degrees of freedom, the number of accessible states of a system still grows combinatorially with the number of valence nucleons. For this reason truncation schemes must be introduced.

In light deformed nuclei the dominance of the quadrupole-quadrupole interaction led to an introduction of the SU(3) shell model [3]. Within the SU(3) algebraic framework, large shell-model spaces can be truncated in a very natural way. While in general realistic interactions mix irreducible representations (irreps) of SU(3), the ground state wavefunction of well-deformed light nuclei are typically dominated by a few SU(3) irreps [4, 5, 6]. The strong spin-orbit interaction renders the SU(3) truncation scheme useless in the heavier nuclei of the *fp*-shell, while at the same time for rare earth and actinide species pseudo-spin emerges as a good symmetry and with it the pseudo-SU(3) model [7, 8, 9].

Pseudo-spin can be recognized from the experimental fact that single-particle orbitals with $j = l - 1/2$ and $j = (l - 2) + 1/2$ in the shell η lie very close in energy and can therefore be labeled as pseudo spin doublets with quantum numbers $\tilde{j} = j$, $\tilde{\eta} = \eta - 1$, and $\tilde{l} = l - 1$. The origin of this symmetry has been traced back to the relativistic mean field equations [10, 11, 12].

In this work the energy spectra and B(E2) transition strengths of ^{159}Tb are calculated from a microscopic perspective using the pseudo SU(3) shell model. Normal parity bands are described in a many-body basis built with active nucleons occupying normal parity levels. Polarization effects due to valence nucleons in intruder orbits are taken into account through the use of effective charges.

Basis states are built from SU(3) irreps obtained by taking the direct product of proton and neutron representations. In [13, 6] it is shown that for a description of the low-energy spectrum of deformed nuclei, the Hilbert

space should be truncated according to contributions of the quadrupole-quadrupole interaction and the single-particle one-body Hamiltonian. While pairing plays a very important role in determining the energy spectrum, but does not strongly modify the wave functions of deformed nuclei.

As can be seen in [14, 15], by using an schematic Hamiltonian parametrized according to systematics [16, 17], it is possible to describe the low-lying energy spectrum of even- and odd-mass heavy deformed nuclei. While the application of the model to other deformed rare-earth and actinide nuclei is in order, in the present contribution we will address some specific questions about the pseudo SU(3) model. In particular, we will discuss the importance of various terms in the Hamiltonian, ways in which their strengths can be deduced from systematic, and the effect each term has on the energy spectra. Taking ^{159}Tb as an example, we will examine the wave functions of each rotational band, paying particular attention to the $B\{E2; J \rightarrow (J-1)\}$ and $B\{E2; J \rightarrow (J-2)\}$ transition strengths between states in the same bands and between states belonging to different bands.

In section 2 the pseudo SU(3) classification scheme is presented. The pseudo SU(3) Hamiltonian and its parametrization is discussed in Section 3. The effect which each term in the Hamiltonian has on the energy spectra is analyzed in Section 4. Section 5 contains the analysis of the wave functions associated with different rotational bands and the associated B(E2) values. Conclusions are discussed in Section 6.

2 The pseudo SU(3) basis

The first step in any application of the pseudo SU(3) model is to build the many-body basis. To do this it is necessary to know how many valence nucleons occupy the normal parity orbitals. We will show how this is done using ^{159}Tb as an example. It has 65 protons and 94 neutrons, and of these, 15 protons and 12 neutrons are in the last unfilled (open) shells. Assuming a deformation $\beta \sim 0.25$, the deformed Nilsson single-particle levels of the active shells are filled from below [18, 19]. Nine protons are distributed in the $1g_{7/2}$ and $2d_{5/2}$ orbitals of the $\eta = 4$ shell, and the remaining six occupy the $1h_{11/2}$ intruder orbital. Eight neutrons occupy the $2f_{7/2}$ and $1h_{9/2}$ orbitals of the $\eta = 5$ shell and four are in $1i_{13/2}$ orbital. The relevant occupation numbers n_π, n_ν can be summarized as

$$n_{\pi}^N = 9, \quad n_{\pi}^A = 6, \quad n_{\nu}^N = 8, \quad n_{\nu}^A = 4 \quad (1)$$

where N refers to normal parity states and A to the abnormal parity (also called unique or intruder) states. The deformed Nilsson mean field is only employed to define the number of nucleons in normal and unique parity orbitals. The use of the pseudo SU(3) basis to describe the normal parity sector implies that these nucleons can occupy all normal parity orbitals, not only those with the lower single particle energies.

As it has been the case for all pseudo SU(3) studies up to now, we will freeze the nucleons in abnormal parity orbital and describe the dynamics using only nucleons in normal parity states. While it has been shown that this is a reasonable, it is nonetheless a strong assumption. This choice is further reflected through the use of effective charges to describe quadrupole electromagnetic transitions which are larger than those usually employed in typical shell-model calculations for light nuclei. A more sophisticated treatment of the problem, with nucleons in intruder orbitals described in the same footing using SU(3) irreps is under development [6].

The many-particle states of n_{α} active nucleons in a given normal parity shell η_{α} , $\alpha = \nu$ or π can be classified by the following chains of groups:

$$\begin{array}{ccccccc} \{1^{n_{\alpha}^N}\} & \{\tilde{f}_{\alpha}\} & \{f_{\alpha}\} & \gamma_{\alpha}(\lambda_{\alpha}, \mu_{\alpha}) & \tilde{S}_{\alpha} & \kappa_{\alpha} & \\ U(\Omega_{\alpha}^N) \supset U(\Omega_{\alpha}^N/2) \times U(2) \supset SU(3) \times SU(2) \supset & & & & & & \\ & \tilde{L}_{\alpha} & & & J_{\alpha}^N & & \\ & & SO(3) \times SU(2) \supset SU_J(2), & & & & \end{array} \quad (2)$$

where above each group the quantum numbers that characterize its irreps are given and γ_{α} and κ_{α} are multiplicity labels of the indicated reductions.

Any state $|J_i M\rangle$, where J is the total angular momentum, M its projection and i an integer index which enumerates the states with the same J, M starting from the one with the lowest energy, is built as a linear combination

$$|J_i M\rangle = \sum_{\beta} C_{\beta}^{JMi} |\beta JM\rangle \quad (3)$$

of the strong coupled proton-neutron states

$$|\beta JM\rangle \equiv |\{\tilde{f}_{\pi}\}(\lambda_{\pi}\mu_{\pi})S_{\pi}, \{\tilde{f}_{\nu}\}(\lambda_{\nu}\mu_{\nu})S_{\nu}; \rho(\lambda\mu)\kappa L, S JM\rangle$$

$$\begin{aligned}
&= \sum_{M_L M_S} (LM_L, SM_S | JM) \sum_{M_{S\pi} M_{S\nu}} (S_\pi M_{S\pi}, S_\nu M_{S\nu} | SM_S) \\
&\quad \sum_{k_\pi \kappa_\nu L_\pi L_\nu M_\pi M_\nu} \langle (\lambda_\pi \mu_\pi) \kappa_\pi L_\pi M_\pi; (\lambda_\nu \mu_\nu) \kappa_\nu L_\nu M_\nu | (\lambda \mu) \kappa L M \rangle_\rho \quad (4) \\
&\quad |\{\tilde{f}_\pi\}(\lambda_\pi \mu_\pi) \kappa_\pi L_\pi M_\pi, S_\pi M_{S\pi}\rangle |\{\tilde{f}_\nu\}(\lambda_\nu \mu_\nu) \kappa_\nu L_\nu M_\nu, S_\nu M_{S\nu}\rangle.
\end{aligned}$$

In the above expression $\langle -; - | - \rangle$ and $(-, - | -)$ are the SU(3) and SU(2) Clebsch Gordan coefficients, respectively. We are considering only configurations with the highest spatial symmetry [6, 20]. For ^{159}Tb the active shells in the pseudo SU(3) space are $\tilde{\eta}_\pi = 3$ and $\tilde{\eta}_\nu = 4$ with degeneracies $\Omega_\pi = 20$ and $\Omega_\nu = 30$, respectively. In the *large* groups $U(10)$ and $U(15)$, the spatially most symmetric irreps for 9 protons and 8 neutrons are, respectively, $\{\tilde{f}_\pi\} = \{2^4 1\}$ and $\{\tilde{f}_\nu\} = \{2^4\}$. It implies that $\tilde{S}_\pi = 1/2$ and $\tilde{S}_\nu = 0$. In other words, we are only taking into account configurations with pseudo spin zero for an even number of nucleons and 1/2 for an odd number of nucleons.

The above considerations rely strongly on the goodness of pseudo-spin symmetry, which manifests itself in the near degeneracy of the pseudo spin-orbit partners. When the *real* SU(3) model is used to describe deformed nuclei in the *pf*-shell, the spin mixing is very important and Eq. (4) must be modified accordingly [6, 21].

What makes the pseudo SU(3) model a powerful theory is that it allows one to invoke a relatively simple and physically motivated basis truncation scheme. Extended shell-model calculations in the *pf*- and *sdg*-shell have shown that in the description of deformed nuclei the Hilbert space can be truncated to only those states that are relevant when both the quadrupole-quadrupole force and the single-particle Hamiltonian are taken into account [13]. While pairing is fundamental to obtaining the correct moment of inertia of the rotational bands, it has a relatively small effect on the overall wave functions [13]. An analysis of the SU(3) content of wave functions obtained in large shell-model diagonalizations [21], as well as the excellent description of ground and excited bands in heavy deformed even- [14, 22] and odd-mass [15] nuclei strongly support this statement.

The quadrupole-quadrupole interaction can be expressed in terms of the second order SU(3) Casimir operator C_2 ,

$$\hat{Q} \cdot \hat{Q} = 4C_2 - 3\hat{L}(\hat{L} + 1). \quad (5)$$

The eigenvalue of C_2 for a given of SU(3) irrep (λ, μ) is given by

$$\langle C_2 \rangle = (\lambda^2 + \mu^2 + \lambda\mu + 3\lambda + 3\mu). \quad (6)$$

The larger the expectation value of C_2 , the greater the binding of that SU(3) irrep by a pure $Q \cdot Q$ interaction. We build the basis selecting the proton and neutron irreps with the largest $\langle C_2 \rangle$.

For ^{159}Tb , the SU(3) representations were selected as follows. Including all the possible spins there are 97 irreps in the proton space and 285 irreps in the neutron space. Proton and neutron irreps which belongs to the irreps $\{\hat{f}_\pi\} = \{2^4 1\}$ and $\{\hat{f}_\nu\} = \{2^4\}$ of the large groups $U(10)$ and $U(15)$, respectively, are found and ordered according to their C_2 value. In Table 1 the seven representations with the largest C_2 in ^{159}Tb are shown.

Table 1

Taking the direct product of these protons and neutrons irreps results in many strong coupled SU(3) irreps. From these, the 15 with the largest C_2 were chosen. They are shown in Table 2. These 15 proton-neutron irreps define the Hilbert space of the model. They are a small subset of all the possible irreps, and involve only 4 proton and 3 neutron irreps. In this strongly truncated space it is possible to describe the low energy spectra of even-even nuclei [14, 22] and normal parity bands in odd-mass nuclei [15]. The validity of the pseudo SU(3) symmetry is the rationale behind this successful truncation scheme.

Table 2.

3 The pseudo SU(3) Hamiltonian

The Hamiltonian contains spherical Nilsson single-particle terms for protons ($H_{sp,\pi}$) and neutrons ($H_{sp,\nu}$), the quadrupole-quadrupole ($\tilde{Q} \cdot \tilde{Q}$) and pairing interactions ($H_{pair,\pi}$ and $H_{pair,\nu}$), as well as three ‘rotor-like’ terms which are diagonal in the SU(3) basis.

$$H = \sum_{\alpha=\pi,\nu} \{H_{sp,\alpha} - G_\alpha H_{pair,\alpha}\} - \frac{1}{2} \chi \tilde{Q} \cdot \tilde{Q} + a K_J^2 + b J^2 + A_{asym} \hat{C}_2. \quad (7)$$

This Hamiltonian can be separated into two parts: the first row includes Nilsson single-particle energies and the pairing and quadrupole-quadrupole interactions (\tilde{Q} is the quadrupole operator in the pseudo SU(3) space, see below). They are the basic components of any realistic Hamiltonian [16, 17] and have been widely studied in the nuclear physics literature, allowing their

respective strengths to be fixed by systematics [16, 17]. In the second row there are three rotor terms used to fine tune the moment of inertia and the position of the different K bands. The SU(3) mixing is due to the single-particle and pairing terms.

The three ‘rotor-like’ terms have been studied in detail in previous papers where the pseudo SU(3) symmetry was used as a dynamical symmetry [18, 19]. In the present work, a and b are the only two parameters used to fit the spectra.

The term proportional to K_J^2 breaks the SU(3) degeneracy of the different K bands [23]. It has the form

$$K_J^2 = \frac{\lambda_1 \lambda_2 J^2 + \lambda_3 X_3^c + X_4^c}{2\lambda_3^c + \lambda_1 \lambda_2} \quad (8)$$

where J^2 , X_3^c and X_4^c are the three rotational scalars formed with products of J and \tilde{Q} and the λ_i coefficients are functions of λ and μ [20, 18, 19], as shown in Appendix A. The reduced matrix elements for X_3^c and X_4^c are evaluated using Racah and SU(3) coupling coefficients [23, 24]. For ^{159}Tb $a = 0.0198$ was found to provide the best fit.

The term proportional to J^2 is used to fine tune the moment of inertia. It represents a small correction to the quadrupole-quadrupole term, which contributes to the rotor spectra with strength $3/2\chi$ (see Eq. (5)). For ^{159}Tb we used $b = -0.0031$, which introduce a change of about 15% in the rotational spectra.

The asymmetry term distinguishes SU(3) irreps with both λ and μ even from the others [25], having no interaction strength in the first case and a positive one in the the second. In this way the contribution of irreps with both λ and μ even is slightly enhanced because they belong to different symmetry types of the intrinsic Vierergruppe D_2 [25]. The asymmetry coefficient has a value $A_{asym} = 0.0008$, fixed according with [24]. The same value was employed for the three A=159 nuclei studied in [15].

The single-particle Nilsson Hamiltonian is

$$H_{sp} = \hbar\omega_0\left(\eta + \frac{3}{2}\right) - \kappa\hbar\omega_0\{2\vec{l} \cdot \vec{s} + \mu\vec{l}^2\}, \quad (9)$$

with parameters [16]

$$\hbar\omega_0 = 41A^{-1/3}[MeV], \quad \kappa_\pi = 0.0637, \quad \kappa_\nu = 0.0637, \quad (10)$$

$$\mu_\pi = 0.60, \quad \mu_\nu = 0.42,$$

The pairing interaction is

$$V_p = -\frac{1}{4}G \sum_{j,j'} a_j^\dagger a_{\bar{j}}^\dagger a_{j'} a_{\bar{j}'}, \quad (11)$$

where \bar{j} denotes the time reversed partner of the single-particle state j and G is the strength of the pairing force. Its second quantized expression in term of SU(3) tensors is reviewed in Appendix B. For the pairing coefficients $G_{\pi,\nu}$, we used [16, 17]

$$G_\pi = \frac{21}{A} = 0.132, \quad G_\nu = \frac{17}{A} = 0.106. \quad (12)$$

In the SU(3) model the collective quadrupole operator, defined by $Q_\mu^c = \sqrt{16\pi/5} \sum_i r_i^2 Y_{2\mu}(\hat{r}_i)/b^2$, is symmetrized in order to correspond to one of the SU(3) generators. It is called the ‘algebraic’ quadrupole operator $Q_\mu^a = \sqrt{4\pi/5} \sum_i [r_i^2 Y_{2\mu}(\hat{r}_i)/b^2 + b^2 p_i^2 Y_{2\mu}(\hat{p}_i)]$ [18, 19]. Within a major oscillator shell, the matrix elements of Q^c and Q^a are identical. When transformed to the pseudo SU(3) basis, it maps to a linear combination of SU(3) tensors which is dominated by the quadrupole operator \tilde{Q} , which is the generator of the pseudo SU(3) algebra [19]. It is this quadrupole operator in the pseudo SU(3) space the one included in the quadrupole-quadrupole interaction in Hamiltonian (7). In first order, the relationship between both quadrupole operators can be written as

$$Q_\mu^a = \frac{\tilde{\eta} + 1}{\tilde{\eta}} \tilde{Q}_\mu \quad (13)$$

which holds for protons and neutrons separately.

The coefficient χ of the operator $\tilde{Q} \cdot \tilde{Q}$ is

$$\chi = \frac{35}{A^{5/3}} = 0.00753. \quad (14)$$

It is consistent with the parametrization discussed in [17], provided one keep in mind that in this reference the quadrupole operator is just $r^2 Y_{2\mu}$, and that, as mentioned above, when operating in the pseudo SU(3) space the interaction must be, in first order, a factor $\left(\frac{\tilde{\eta}+1}{\tilde{\eta}}\right)^2$ stronger than the similar

one in the normal space. This implies that the constant χ in [17] is a factor $\frac{16\pi/5}{[(\bar{\eta}+1)/\bar{\eta}]^2} \approx 6.5$ larger than our χ .

The electric quadrupole operator is expressed as[20]

$$Q_\mu = e_\pi Q_\pi + e_\nu Q_\nu \approx e_\pi \frac{\eta_\pi + 1}{\eta_\pi} \tilde{Q}_\pi + e_\nu \frac{\eta_\nu + 1}{\eta_\nu} \tilde{Q}_\nu, \quad (15)$$

with effective charges $e_\pi = 2.3$, $e_\nu = 1.3$. These values are very similar to those used in the pseudo SU(3) description of even-even nuclei [20, 14]. They are larger than those used in standard calculations of B(E2) strengths [16] due to the passive role assigned to the nucleons in unique parity orbitals, whose contribution to the quadrupole moments is parametrized in this way.

4 The energy spectra

Fig. 1 shows the yrast and excited bands in ^{159}Tb . Experimental data [26] are plotted on the left hand side, while those obtained using the Hilbert space and the Hamiltonian parameters discussed in the previous sections are shown in the right hand side. The agreement between both is excellent, as is the case for the nuclei ^{159}Eu and ^{159}Dy , whose energy spectra was studied in [15]. From the four bands reported in the literature in ^{159}Tb , three of them (the yrast, $5/2_1^+$, and $3/2_2^+$ bands) have a difference between the experimental and predicted levels of less than 50 KeV. The $1/2_1^+$ is slightly high in energy, and the model predicts an exaggerated staggering, with origin discussed below.

Figure 1

The whole energy spectra is built up by the interplay between the single-particle and quadrupole-quadrupole terms in the Hamiltonian [13, 6]. These two terms define the relative ordering between the different bands, as well as the main components of the wavefunction. As expected, the use of realistic single-particle energies plays a key role in the appropriate description of odd-mass nuclei.

To make this point clear, in Fig. 2 the theoretical energy spectra calculated with Hamiltonian (7) *without single-particle energies* are presented on the right of each column and compare it with the corresponding experimental energies on the left of each column [26]. It is clear that the ordering is shifted. The ground state is now predicted to have $J = \frac{1}{2}$, the first excited band starts with $J = \frac{5}{2}$. Only the third band with $J = \frac{3}{2}$ remains ordered correctly. The wave functions of all the states in all these three bands are dominated

(more than 95%) by the leading SU(3) irrep $(28, 8), (10, 4)_\pi(18, 4)_\nu$. We will return to this point when discussing the wave functions in Section 5.

Figure 2

From Fig. 2 it is also clear that, in absence of single-particle energies, the quadrupole-quadrupole interaction rules over all the others, even in the presence of realistic pairing strengths. It determines the single SU(3) irrep that dominates the low energy spectra and the rotor pattern each band exhibits.

In order to discuss the effect each of the remaining term in Hamiltonian (7) has on the energy spectra, three rotational bands are plotted in Figure 3: the yrast band in insert (a), the $5/2_1^+$ band in insert (b) and the $1/2_1^+$ band in insert (c). In the first column from the left the experimental energies are plotted for each band, with the angular momentum and parity of each state written on the left. The next column presents the theoretical results, the same ones shown in Fig. 1. The next three columns show the theoretical spectra obtained *without* the pairing interaction (third column, $G_\pi = G_\nu = 0$), without pairing between protons (fourth column, $G_\pi = 0$) and without pairing between neutrons (fifth column, $G_\nu = 0$). The remaining four columns depict the behavior of the spectra when the rotor terms are turned off. The sixth column, labeled K^2 , shows the spectra without this term ($a = 0$), the seventh column without the J^2 term ($b = 0$), the eighth without the asymmetry term ($A_{asym} = 0$) and the ninth presents the spectra with all the three rotor terms turned off ($a = b = A_{asym} = 0$). The last column on the right presents the experimental energies again, to help with the comparison.

Figure 3

The theoretical description of the yrast band is good. The effect of the pairing interaction is clearly seen in the third column; namely, it expands the energy spectra. This is a rather remarkable result that seems to come about because of the highly truncated nature of the basis. The pairing interaction strongly mixes the SU(3) irreps [27, 28, 29, 30] and plays an important role in determining the moment of inertia of this deformed nuclei. At the same time its effects on the wavefunction are minor, as has been discovered in independent shell-model calculations [13]. Comparing the third, fourth and fifth columns, it is clear it is the pairing interaction between neutrons that is most important. The last uncoupled proton in ^{159}Tb seems to nearly ignore the effect of pairing. The K^2 term has negligible effect on the yrast band. The J^2 term helps to fine tuning the moment of inertia to the experimental number. The asymmetry term pushes the $J = \frac{17}{2}$ state down in energy and

closer to the experimental value. Although a small contribution it is clearly important and provides justification for including this term included in the Hamiltonian.

The $5/2_1$ band shown in insert (b) shows a similar behavior. The first three states reported are in close agreement with the experimental data, and theory predicts more states that belongs to this band. In the absence of pairing, the energy spectra is compressed which is due mainly to the protons. The K^2 term is clearly relevant for this band: when it is missing the band head moves down about 100 KeV in energy. The J^2 term modifies the moment of inertia slightly.

The $1/2_1$ band is shown in insert (c). Its band head is predicted at an energy 150 KeV larger than the measured one. The theory predicts three nearly degenerated pairs of levels: $(\frac{3}{2}, \frac{5}{2})$, $(\frac{7}{2}, \frac{9}{2})$ and $(\frac{11}{2}, \frac{13}{2})$ while their experimental counterparts are less closely packed. As can be seen in the eighth column, when $A_{asym} = 0$ the level spacing is closer to the reported one, but the band-head energy is too high. It is noticeable that turning off the K^2 term the energies move upwards, while in the $5/2_1$ band they move downward.

The contribution of each term in the Hamiltonian can be summarized as follows:

- **Quadrupole-quadrupole:** This interaction is tied to the quadrupole deformation, and since the pioneering work of Elliott [3] has been known to play a crucial role in the dynamics of deformed nuclei. In the pseudo SU(3) model its dominance can also be used to determine the truncation of the Hilbert space.
- **Spherical single-particle energies:** These form the basis of the shell model, and serve to define the low-energy spectra of odd-mass nuclei. And this is precisely the role they play in the pseudo SU(3) model: they determine to a large extent the relative ordering of the different bands. Together with the quadrupole-quadrupole interaction, the single-particle energies define the gross features of the energy spectra and the mixing of different SU(3) irreps in the wave functions.
- **Pairing:** This interaction expands the whole energy spectra, almost as though it is a multiplicative constant in front of the Hamiltonian (7). It also shifts the energy of each band head and alters the moment of inertia of each band. The success of previous investigations that used the pseudo SU(3) symmetry as a dynamical symmetry [18, 19] without the mixing

of SU(3) representations, is partially a result of this effect: a larger quadrupole-quadrupole and rotor strength mimics the effect of pairing on the spectra. The pairing interaction acting in the subspace with an odd number of nucleons has a nearly negligible effect on the low-lying bands. The subspace with even number of nucleons is responsible for most of the pairing effects.

- **K^2 :** Since it has been shown that this particular combination of 2-, 3- and 4-body terms corresponds to the square of the third component of the angular momentum in the intrinsic frame [25], it can be used to adjust band-head energies. For the $5/2_1$ band, when $a = 0$ the band-head energy is 277 keV, while in the presence of this term it moves up to 356 keV, which is close to the experimental value of 348 keV [26].
- **J^2 :** This diagonal term provides small corrections to the moment of inertia. The negative b value used in the present study makes serves to increase the moment of inertia, compressing the corresponding spectra.
- **Asymmetry:** This term enhances the contribution of the SU(3) irreps with both λ and μ even. It has an important effect on states with large angular momentum. For example, in the absence of this term the state $\frac{17}{2}^+$ of the yrast band is displaced to higher energies due to mixing with other SU(3) irreps with λ or μ odd.
- **Rotor terms:** The effect of suppressing simultaneously the three rotor terms, *i.e.* taking $a = b = A_{asym} = 0$, is shown in the ninth column of Fig. 3. The inclusion of Nilsson single-particle energies and the pairing and quadrupole-quadrupole interactions suffices to provide a very reasonable energy spectra, with all known bands in their correct order and the overall rotor features reproduced. The rotor terms provide the fine tuning, with energies being adjusted by no more than 15 %. The predictive power of the pseudo SU(3) model strongly relies in this fact.

5 B(E2) transition strengths and wave functions

Up to this point we have centered the discussion on the energetics. But the pseudo SU(3) model is far more powerful than this, it can also success-

fully describe the electromagnetic transitions. Most of the B(E2) transition strengths between states in the first four bands in ^{159}Tb are presented in Fig. 4 for the $J \rightarrow J - 1$ transitions, and in Fig. 5 for the $J \rightarrow J - 2$ transitions.

Figure 4

Figure 5

Calculated B(E2) values are given in units of $e^2b^2 \times 10^{-2}$. They are written close to the arrow which graphically show the transition they describe. The effective charge employed was discussed in relation with Eq. (15). This is the only extra parameter introduced, and has a value very close to those used in previous studies [19]. To assess the quality of the results, the experimental B(E2) values [26] between yrast band states are reported in Table 3. Most of the transition strengths are reproduced within the experimental error bars. One exception is the transition $17/2_1 \rightarrow 13/2_1$ which is underestimated. This could be related with the change in the wavefunction of the first $\frac{17}{2}$, whose mixing with the second $\frac{17}{2}$ state seems to be exaggerated in the model, as discussed below.

Table 3

Notice that while the intraband B(E2) transition strengths are on the order of hundreds $e^2b^2 \times 10^{-2}$, the interband transitions are much less, typically on the order of $e^2b^2 \times 10^{-2}$ or fractions thereof. This fact supports the identification of states belonging to bands, and is consistent with the wavefunction analysis. The only measured interband transition is the $1/2_1 \rightarrow 5/2_1$ and it too is well reproduced by the model, which predicts a value of $2.96 e^2b^2 \times 10^{-2}$.

It is very instructive to analyze the wave functions of the states belonging to the lowest lying energy bands obtained with the Hamiltonian (7). The nine most important SU(3) irreps which are relevant to the description of these bands are listed in Table 4.

Table 4

In Figure 6 the percentage each irrep contributes to each state is plotted as a function of the angular momentum of the state for the different bands. These were calculated from the wavefunctions, Eq. (3), as simply $100 \times |C_\beta^{JMi}|^2$. The symbols listed in the first column of Table 4 identifies the various components. All contributions larger than 2 % are plotted, and in all cases the states shown add up to at least 95% of the total wavefunction.

Figure 6

Each insert, (a) to (d) in Figure 6, gives the main components of one of the bands plotted in Figs. 4 and 5, from the band head and up to the state with $J = \frac{15}{2}$ or $\frac{17}{2}$. As shown, all have a very regular structure as one moves

up the bands. While in all the cases there is strong mixing of SU(3) irreps, the mixing remains nearly the same for the states with different angular moments belonging to the same band. In this sense the mixing is *adiabatic* within each band. This coherence explains the large B(E2) values for intra-band transitions.

In insert (a) the components of each state belonging to the $3/2_1$ band are shown. As shown, the states from $J^\pi = 3/2^+$ to $17/2^+$ are about 30 % $(30, 4)[(10, 4)_\pi \times (20, 0)_\nu]$, 29 % $(28, 8)[(10, 4)_\pi \times (18, 4)_\nu]$, 14 % $(30, 4)[(11, 2)_\pi \times (18, 4)_\nu]$, 12 % $(31, 2)[(11, 2)_\pi \times (20, 0)_\nu]$ with smaller contributions from the $(31, 2)$ and $(29, 6)$ representations that are almost constant for all the states in the band.

States in the $5/2_1$ band, insert (b), have about 36 % $(28, 8)[(10, 4)_\pi \times (18, 4)_\nu]$, 22 % $(30, 4)[(11, 2)_\pi \times (18, 4)_\nu]$, and 20 % $(30, 4)[(10, 4)_\pi \times (20, 0)_\nu]$ which decreases to less than 15% for the $J = \frac{15}{2}$ state. Other irreps contribute less than 10% each. The $1/2_1$ band, insert (c), is the purest of the four considered. It has around 60 % $(28, 8)[(10, 4)_\pi \times (18, 4)_\nu]$, 20% $(30, 4)[(11, 2)_\pi \times (18, 4)_\nu]$, and 10 % $(30, 4)[(10, 4)_\pi \times (20, 0)_\nu]$. It is interesting to note that this band becomes the ground state band when the single-particle energies are not present (see the discussion below Figure 2), and in that case all the states in the four bands are built primarily out of the $(28, 8)[(10, 4)_\pi \times (18, 4)_\nu]$ irrep.

The $3/2_2$ band, insert (d), is dominated by the irrep $(30, 4)[(10, 4)_\pi \times (18, 4)_\nu]$ which get strongly mixed with the $(28, 8)[(10, 4)_\pi \times (18, 4)_\nu]$ for $J = \frac{11}{2}$ and $\frac{13}{2}$.

As was mentioned above, the interplay between the single-particle and the quadrupole-quadrupole terms in the Hamiltonian defines the SU(3) mixing in the wave functions. The four bands discussed here have strong mixing, and the ground state band is *not* dominated by the leading irrep, the one which would constitute the ground band in the pure SU(3) symmetry limit. The delicate balance between these two interactions, whose strengths are taken from known systematics and not used as fitting parameters, defines the gross features of the calculated energy spectra which are found to be in good agreement with the available experimental information.

Although the basis is strongly truncated, being built from the 15 SU(3) irreps listed in Table 2, not even all of these play an important role. The low-lying energy bands discussed above are dominated by the irreps coming from the first four rows in Table 2, which are combinations of the two proton SU(3) irreps $(10, 4)_\pi$ and $(11, 2)_\pi$ and the two neutron SU(3) irreps $(18, 4)_\nu$

and $(20, 0)_\nu$.

6 Conclusions

We have shown that the normal parity bands in the odd-mass heavy deformed nuclei with $A = 159$ can be described quantitatively using the pseudo SU(3) model [15]. A careful examination of the wave functions and B(E2) transition strengths for the four low-lying energy bands in ^{159}Tb was made, analyzing their structure in terms of their SU(3) components, and relating them with their intra- and inter-band transitions, for which the calculated values agree closely with the known experimental numbers.

The most relevant feature of the present application of the pseudo SU(3) model is a determination of the primary features of the energy spectra of the normal parity rotational bands in ^{159}Tb using a Hamiltonian with Nilsson single-particle energies and quadrupole-quadrupole and pairing interactions with strengths fixed by systematics – strengths of the primary interactions were *not* varied to obtain a “best fit” to the data. A few extra rotor-like terms were used to obtain a more precise description of the energies and B(E2) values, but this “fine tuning” not affect the spectra in a major way and had little influence on the structure of the calculated wavefunctions.

This work shows the pseudo SU(3) model to be a powerful shell-model scheme, one that can be used to describe normal parity bands in deformed rare-earth and actinide isotopes by performing a symmetry dictated truncation of the Hilbert space and using a systematic parametrization of the dominant terms in the Hamiltonian. It opens up the possibility of a detailed microscopic analysis of other nuclear properties of heavy deformed nuclei, both with even and odd numbers of protons and neutrons, like g-factors, M1 transitions and beta decays.

7 Acknowledgments

This work was supported in part by Conacyt (México) and the U.S. National Science Foundation, the latter being through Grants 9500474 and 9603006, as well as an NSF Cooperative Agreement, 9720652, that includes matching from the Louisiana Board of Regents Support Fund.

Appendix A: The K_J^2 term

The residual interaction, K^2 , is a linear combination of J^2 , X_3 and X_4 , which are rotational scalar operators built from generators of the $SU(3)$ algebra, that is [18, 19],

$$\begin{aligned} J^2 &= \sum_i^3 J_i^2 \\ X_3 &= \sum_{i,j}^3 J_i Q_{ij}^a J_j \end{aligned} \quad (16)$$

$$X_4 = \sum_{i,j,k}^3 J_i Q_{ij}^a Q_{jk}^a J_k \quad (17)$$

where J_i and Q_{ij}^a are cartesian forms of the total angular momentum and the quadrupole operators, respectively. The K is interpreted to be the third component of the total angular momentum along the intrinsic body-fixed symmetry axis of the system, which is given by [18, 19]

$$K^2 = (\lambda_1 \lambda_2 J^2 + \lambda_3 X_3 + X_4) / (2\lambda_3^2 + \lambda_1 \lambda_2), \quad (18)$$

with the parameters λ_i denoting the eigenvalues of the mass quadrupole operator, which are related to the $SU(3)$ labels (λ, μ) through the expressions [31, 23].

$$\lambda_1 = \frac{1}{3}(\mu - \lambda), \quad \lambda_2 = -\frac{1}{3}(\lambda + 2\mu + 3), \quad \lambda_3 = \frac{1}{3}(2\lambda + \mu + 3). \quad (19)$$

The last expressions can be obtained by requiring a linear correspondence between the invariants of the $SU(3)$ and the semidirect product $T_5 \wedge SO(3)$ groups [31, 23]. Indeed, the expectation value of the operator (18), with respect to an orthonormalized basis associated to the chain of groups $SU(3) \rightarrow SO(3)$, corresponds to the eigenvalues of the third component of an intrinsic angular momentum when $L \ll \min(\lambda, \mu)$.

Appendix B: The pairing interaction

The pairing term (11) in the Hamiltonian can be expressed in second quantization as [27, 28]

$$\begin{aligned} V_p &= \frac{G}{2} \sum_{(\lambda_1, \mu_1)(\lambda_2, \mu_2)} \sum_{\eta\eta'} P_{\eta\eta'} \{(\lambda_1, \mu_1)(\lambda_2, \mu_2)\rho_0(\lambda_0, \mu_0)\} \\ &\quad [[a_\eta^\dagger \otimes a_\eta^\dagger]^{\lambda_1 \mu_1} \otimes [\tilde{a}_{\eta'} \otimes \tilde{a}_{\eta'}]^{\lambda_2 \mu_2}]^{\rho_0 \lambda_0 \mu_0 k_0=1 l_0=s_0=0} \end{aligned} \quad (20)$$

where

$$P_{\eta\eta'}\{(\lambda_1, \mu_1)(\lambda_2, \mu_2)\rho_0(\lambda_0, \mu_0) = \sum_{l'} \sqrt{(2l+1)(2l'+1)} \langle(\eta, 0)l; (\eta, 0)l || (\lambda_1, \mu_1)10\rangle \quad (21)$$

$$\langle(\eta', 0)l'; (\eta', 0)l' || (\lambda_2, \mu_2)10\rangle \langle(\lambda_1, \mu_1)10; (\lambda_2, \mu_2)10 || (\lambda_0, \mu_0)10\rangle\}. \quad (22)$$

References

- [1] M. G. Mayer, Phys. Rev. **75** (1949) 1969; O. Haxel, J. H. D. Janssen and H. E. Suess, Phys. Rev. **75** (1949) 1766.
- [2] B. A. Brown and B. H. Wildenthal, Ann. Rev. Nucl. Part. Sc. **38** (1988) 29; E. Caurier, J. L. Egido, G. Martínez Pinedo, A. Poves, J. Retamosa, L. M. Robledo and A. P. Zuker, Phys. Rev. Lett. **75** (1995) 2466.
- [3] J. P. Elliott, Proc. Roy. Soc. London Ser. A **245** (1958) 128; **245** (1958) 562.
- [4] Y. Akiyama, A. Arima and T. Tebe, Nucl. Phys, **A 138** (1969) 273.
- [5] J. Retamosa, J.M. Udías, A. Poves and E. Moya de Guerra, Nucl. Phys. **A 511** (1990) 221; D. Troltenier, J. P. Draayer and J.G. Hirsch, Nucl. Phys. **A 601** (1996) 89.
- [6] C. Vargas, J. G. Hirsch, P. O. Hess and J. P. Draayer, Phys. Rev. **C 58** (1998) 1488.
- [7] K. T. Hecht and A. Adler, Nucl. Phys. **A 137** (1969) 129.
- [8] A. Arima, M. Harvey and K. Shimizu, Phys. Lett. **B 30** (1969) 517.
- [9] R. D. Ratna Raju, J. P. Draayer and K. T. Hetch, Nucl. Phys. **A 202** (1973) 433 .
- [10] A. L. Blokhin, C. Bahri and J. P. Draayer, Phys. Rev. Lett. **74** (1995) 4149.
- [11] J. N. Ginocchio, Phys. Rev. Lett. **78** (1997) 436.

- [12] J. Meng, K. Sugawara-Tanabe, S. Yamaji, P. Ring and A. Arima, Phys. Rev. **C 58** (1998) R632.
- [13] A. P. Zuker, J. Retamosa, A. Poves and E. Caurier, Phys. Rev. **C 52** (1995) R1741.
- [14] T. Beuschel, J. P. Draayer, D. Rompf and J.G. Hirsch, Phys. Rev. **C 57** (1998) 1233.
- [15] C. Vargas, J. G. Hirsch, T. Beuschel and J. P. Draayer, Phys. Rev. **C 61** (2000) 031301(R).
- [16] P. Ring and P. Schuck. *The Nuclear Many-Body Problem*, Springer, Berlin (1979).
- [17] M. Dufour and A. P. Zuker, Phys. Rev. **C 54** (1996) 1641.
- [18] J. P. Draayer and K. J. Weeks, Ann. of Phys. **156** (1984) 41.
- [19] O. Castaños, J. P. Draayer and Y. Leschber, Ann. of Phys. **180** (1987) 290.
- [20] J. P. Draayer, K. J. Weeks and K. T. Hetch, Nucl. Phys. A **381** (1982) 1.
- [21] J. G. Hirsch, P. O. Hess, L. Hernández, C. Vargas, T. Beuschel and J.P. Draayer, Rev. Mex. Fis. **45** supl 2 (1999) 86.
- [22] T. Beuschel, J. G. Hirsch and J. P. Draayer, Phys. Rev. **C** submitted.
- [23] H. A. Naqvi and J. P. Draayer, Nucl. Phys. **A 516** (1990) 351; **A 536** (1992) 297.
- [24] Doctoral Thesis, Thomas Beuschel, 1998. LSU
- [25] Y. Leschber, Hadronic Journal Supplement **3** (1987) 1.
- [26] National Nuclear Data Center, <http://bnlnd2.dne.bnl.gov>
- [27] D. Troltenier, C. Bahri and J. P. Draayer, Nucl. Phys. **A 586** (1995) 53; **A 589** (1995) 75.

- [28] C. Bahri, J. Escher and J. P. Draayer, Nucl. Phys. **A 592** (1995) 171;
A 594 (1995) 485.
- [29] J. Escher, C. Bahri, D. Troltenier and J. P. Draayer, Nucl. Phys. **A 633**
(1998) 662.
- [30] C. Bahri, D. J. Rowe and W. Wijesundera, Phys. Rev. **C 58** (1998)
1539.
- [31] O. Castaños, J. P. Draayer and Y. Leschber, Z. Phys. **329** (1988) 33.

Table Captions

Table 1: Irreps and C_2 values for protons and neutrons in ^{159}Tb . Only the seven irreps with largest C_2 values are listed .

Table 2: The 15 pseudo SU(3) irreps used in the description of ^{159}Tb bands.

Table 3: Experimental B(E2) transition strengths for ^{159}Tb .

Table 4: Explicit form of the irreps referred to as the components of the wavefunctions in Figure 6.

(λ_π, μ_π)	C_2	(λ_ν, μ_ν)	C_2
(10,4)	198	(18,4)	478
(7,7)	189	(20,0)	460
(11,2)	186	(16,5)	424
(2,11)	186	(17,3)	409
(8,5)	168	(18,1)	400
(5,8)	168	(13,8)	400
(9,3)	153	(14,6)	376

Table 1

(λ_π, μ_π)	(λ_ν, μ_ν)	total (λ, μ)					
(10,4)	(18,4)	(28,8)	(29,6)	(30,4)	(31,2)	(32,0)	(26,9)
(11,2)	(18,4)	(29,6)	(30,4)	(31,2)			
(10,4)	(20,0)	(30,4)					
(11,2)	(20,0)	(31,2)					
(7,7)	(18,4)	(25,11)	(26,9)				
(10,4)	(16,5)	(26,9)					
(8,5)	(18,4)	(26,9)					

Table 2

Experimental B(E2) for ^{159}Tb	
$J_{\#}^+ \rightarrow (J-2)_{\#}^+$	Exp [$e^2 b^2 \times 10^{-2}$]
$7/2_1^+ \rightarrow 3/2_1^+$	73.7 ± 10.2
$9/2_1^+ \rightarrow 5/2_1^+$	111.5 ± 6.1
$11/2_1^+ \rightarrow 7/2_1^+$	147.9 ± 3.6
$13/2_1^+ \rightarrow 9/2_1^+$	166.3 ± 4.6
$15/2_1^+ \rightarrow 11/2_1^+$	158.1 ± 10.7
$17/2_1^+ \rightarrow 13/2_1^+$	154.5 ± 10.2
$1/2_1^+ \rightarrow 5/2_1^+$	2.56

$J_{\#}^+ \rightarrow (J-1)_{\#}^+$	Exp [$e^2 b^2 \times 10^{-2}$]
$5/2_1^+ \rightarrow 3/2_1^+$	186.7 ± 9.7
$7/2_1^+ \rightarrow 5/2_1^+$	117.7 ± 25.6
$9/2_1^+ \rightarrow 7/2_1^+$	59.9 ± 6.6
$11/2_1^+ \rightarrow 9/2_1^+$	57.3 ± 5.6
$13/2_1^+ \rightarrow 11/2_1^+$	32.2 ± 4.1
$15/2_1^+ \rightarrow 13/2_1^+$	38.4 ± 6.6

Table 3

labels and irreps for ^{159}Tb			
<i>label</i>	$(\lambda, \mu)_T S_T$	$(\lambda_{\pi}, \mu_{\pi}) S_{\pi}$	$(\lambda_{\nu}, \mu_{\nu}) S_{\nu}$
†	$(30, 4)_{\frac{1}{2}}$	$(10, 4)_{\frac{1}{2}}$	$(20, 0)0$
◇	$(28, 8)_{\frac{1}{2}}$	$(10, 4)_{\frac{1}{2}}$	$(18, 4)0$
★	$(30, 4)_{\frac{1}{2}}$	$(11, 2)_{\frac{1}{2}}$	$(18, 4)0$
◁	$(31, 2)_{\frac{1}{2}}$	$(11, 2)_{\frac{1}{2}}$	$(20, 0)0$
●	$(31, 2)_{\frac{1}{2}}$	$(10, 4)_{\frac{1}{2}}$	$(18, 4)0$
*	$(29, 6)_{\frac{1}{2}}$	$(11, 2)_{\frac{1}{2}}$	$(18, 4)0$
○	$(29, 6)_{\frac{1}{2}}$	$(10, 4)_{\frac{1}{2}}$	$(18, 4)0$
×	$(30, 4)_{\frac{1}{2}}$	$(10, 4)_{\frac{1}{2}}$	$(18, 4)0$
▷	$(31, 2)_{\frac{1}{2}}$	$(11, 2)_{\frac{1}{2}}$	$(18, 4)0$

Table 4

Figure Captions

Fig. 1: Experimental (left hand side) and theoretical (right hand side) energies for the first four bands in ^{159}Tb .

Fig. 2: Experimental (left hand side) and theoretical (right hand side) energies calculated *without* single-particle energies.

Fig. 3: Energy bands in ^{159}Tb . The first and tenth columns depict the experimental spectra. The second column shows the spectra obtained using Hamiltonian (7). The next seven columns show the same spectra obtained using Hamiltonian (7) but with one term neglected, which is identified below each column: the third column does not include pairing, the fourth column does not include proton pairing, the fifth column does not include neutron pairing, the sixth column does not include the K_J^2 term, the seventh column does not include the J^2 term, the eighth eighth column does not include the asymmetry term, and finally, the ninth column does not include any of the three rotor terms. Insert (a) shows the $3/2_1$ band, insert (b) the $5/2_1$ band and insert (c) the $1/2_1$ band.

Fig. 4: ^{159}Tb theoretical energies and $B\{E2; J \rightarrow (J - 1)\}$ transition strengths (in units $e^2 b^2 \times 10^{-2}$). The latter are written close to the arrows indicating each transition.

Fig. 5: ^{159}Tb theoretical energies and $B\{E2; J \rightarrow (J - 2)\}$ transition strengths, with the same convention as for Fig. 4.

Fig. 6: $\text{SU}(3)$ components of the calculated eigenstates in the first four bands of ^{159}Tb . The angular momentum is listed in the horizontal axis. The symbols refer to the first column in Table 4. Insert (a) shows the $3/2_1$ band, insert (b) the $5/2_1$ band, insert (c) the $1/2_1$ band and insert (d) the $3/2_2$ band.

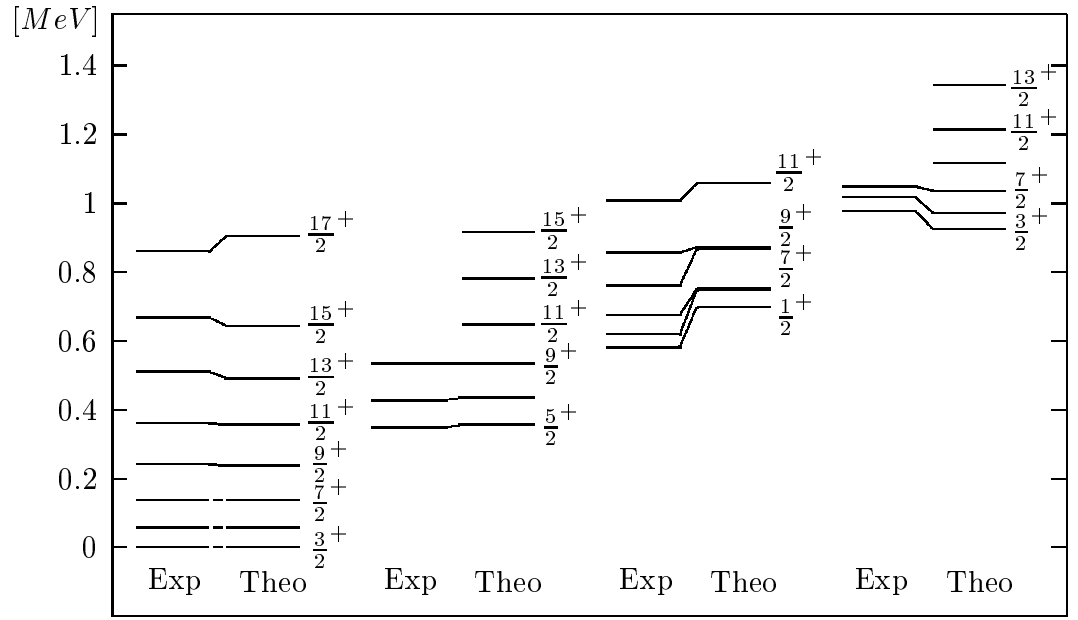


Fig. 1

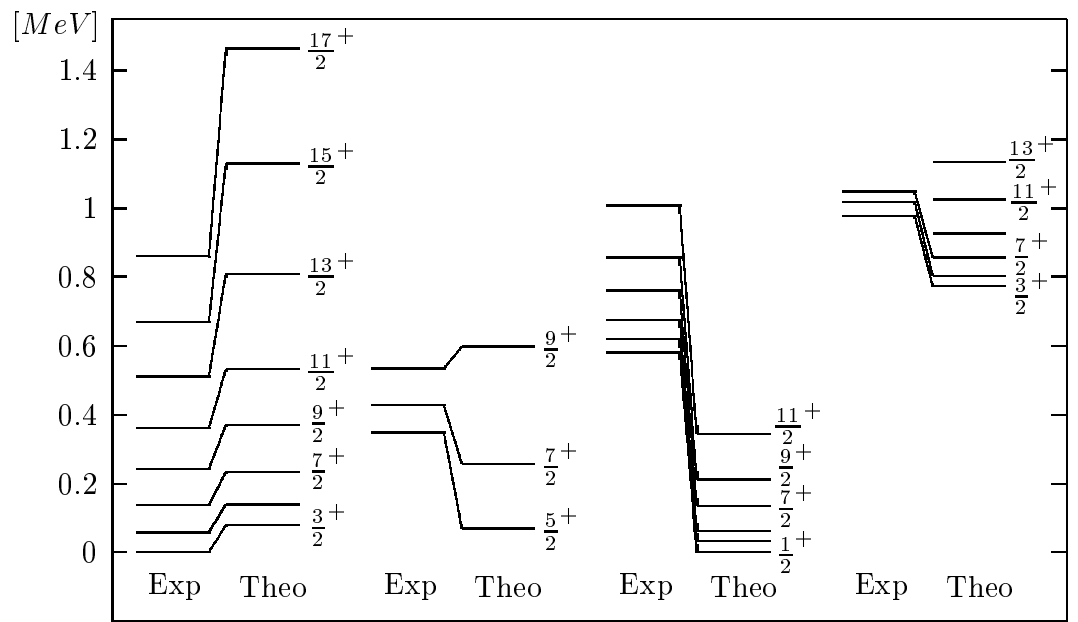


Fig. 2

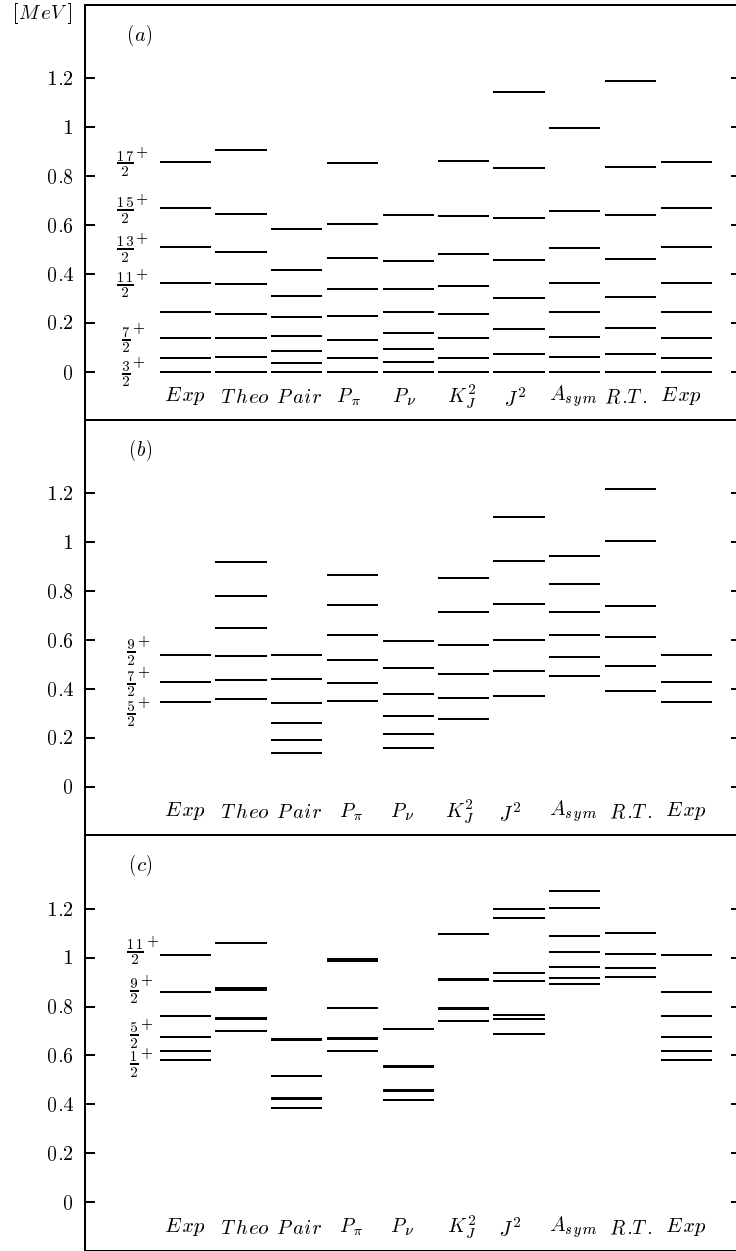
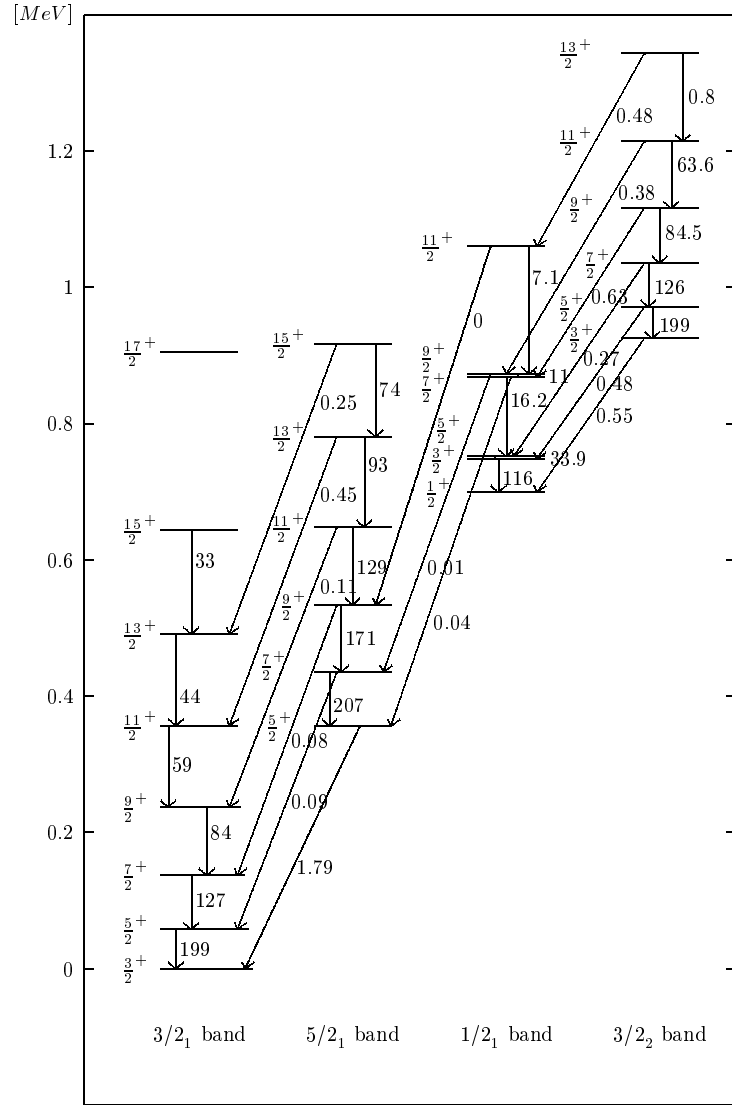


Fig. 3



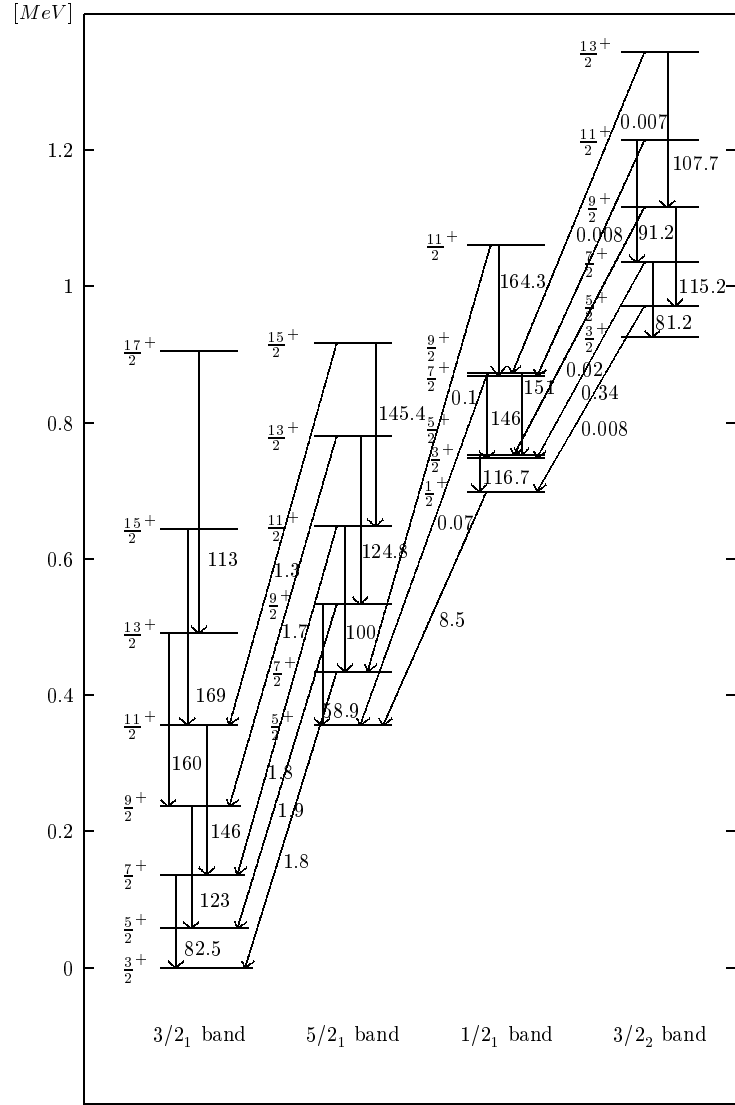


Fig. 5

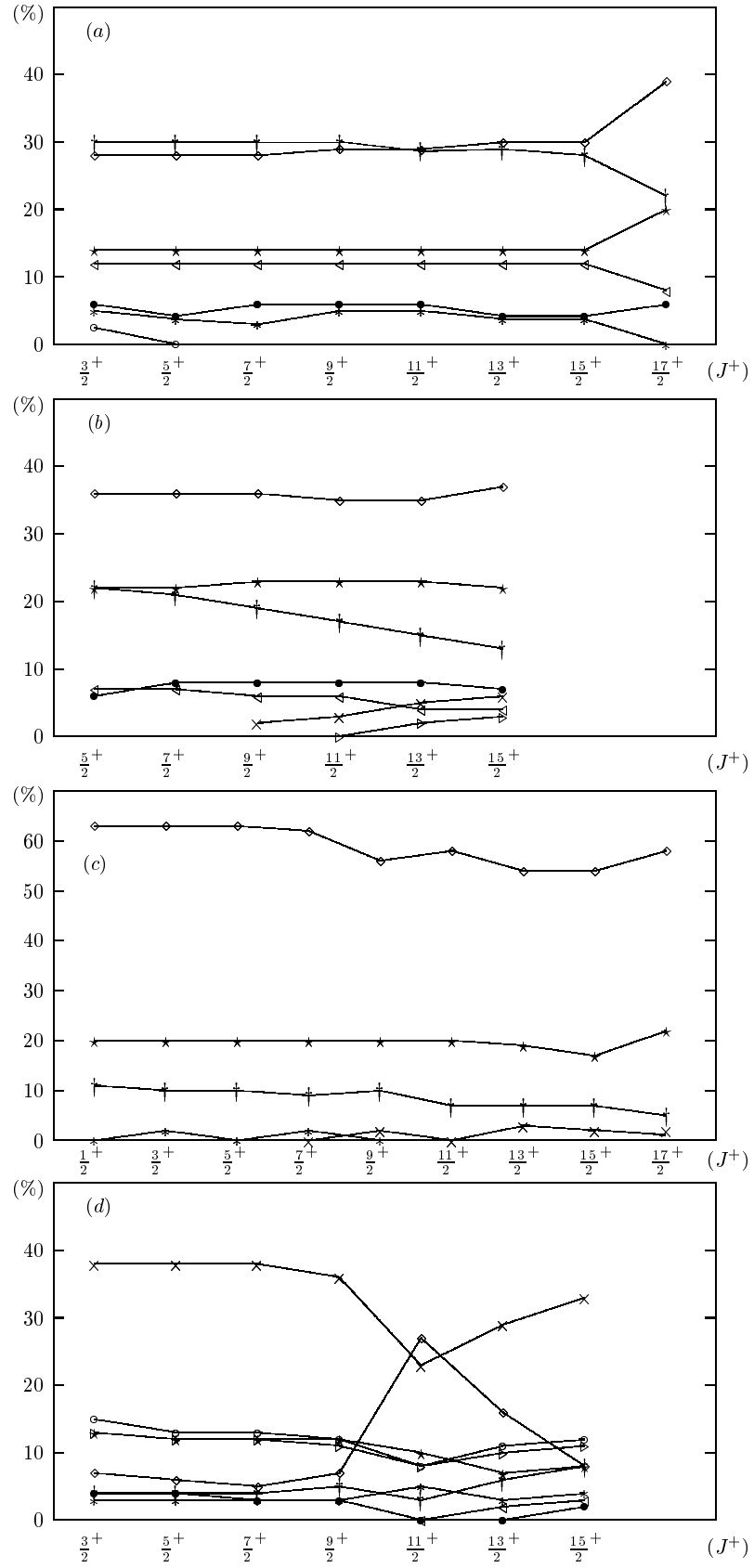


Fig. 6